High- and low-emissions scenario projections of the Southern Hemisphere storm track

Isaac Campbell[1] and James Arthur Renwick[2]

[1]Te Herenga Waka - Victoria, University of Wellington
[2]Victoria University of Wellington

May 13, 2023

Abstract

The Southern Hemisphere storm track is a key component of the Earth's global circulation patterns, with a prominent role in the movement of heat and momentum across the mid-latitudes, and a controlling influence over the behaviour of synoptic eddies. Storm track characteristics are expected to change with anthropogenic forcings, leading to changes in regional weather patterns, and impacting communities through its influence on extreme events. We document projected storm track climatologies at the end of the 21st century under high- and low-emissions scenarios using the CMIP6 generation of models. We find previously described projections – the poleward migration of the storm track, and intensification of storm activity – persist in CMIP6. We explore projections of spatio-temporal variability of the Southern Annular Mode, and consequences for the storm track.

High- and low-emissions scenario projections of the Southern Hemisphere storm track

I. Campbell[1], J. Renwick[1]

[1]Te Herenga Waka - Victoria, University of Wellington

Key Points:

- We find increased storm track activity across the Southern Hemisphere is projected to scale with emissions.
- Similar to previous generations, CMIP6 models predict a poleward migration of the Southern Hemisphere storm track.
- The role of the Southern Annular Mode doesn't change significantly with continued anthropogenic forcing.

Corresponding author: Isaac Campbell, `isaac.campbell6@googlemail.com`

Abstract

The Southern Hemisphere storm track is a key component of the Earth's global circulation patterns, with a prominent role in the movement of heat and momentum across the mid-latitudes, and a controlling influence over the behaviour of synoptic eddies. Storm track characteristics are expected to change with anthropogenic forcings, leading to changes in regional weather patterns, and impacting communities through its influence on extreme events. We document projected storm track climatologies at the end of the 21st century under high- and low-emissions scenarios using the CMIP6 generation of models. We find previously described projections – the poleward migration of the storm track, and intensification of storm activity – persist in CMIP6. We explore projections of spatio-temporal variability of the Southern Annular Mode, and consequences for the storm track.

Plain Language Summary

Weather in the Southern Hemisphere is heavily influenced by the storm track, with extreme events in the mid-latitudes closely linked to passing storms. As the Earth's climate changes with continued greenhouse gas emissions, understanding how the storm track will change is vital to make effective efforts to adapt. We show that state-of-the-art models indicate storm activity is set to increase, likely leading to more frequent extreme weather where storms occur.

1 Introduction

The storm track: past, present, and future

The global climate is a complex system; a web of tensions and feedbacks that make its evolution difficult to predict in detail. The Earth's climate tends toward a state of equilibrium; however, human-induced changes have caused a shift in the basic state (Eyring et al., 2021). Primarily, CO_2 emissions alter atmospheric chemistry, leading to an altered radiative budget. As the climate tends toward a new equilibrium, forced changes will impact components of the Earth system, such as the storm tracks.

The Southern Hemisphere (SH) storm track influences hemispheric circulation patterns, and properties of synoptic eddies, which directly impact human lives and livelihoods (Pfahl & Wernli, 2012). Storm track characteristics exhibit trends over the historical record. Several studies suggest there has been a poleward migration of the mean storm track position (Pena-Ortiz et al., 2013), an increase in the extreme storm frequency (Reboita et al., 2015; Wang et al., 2016), and in eddy kinetic energy (EKE) (Chemke et al., 2022). Studies find these trends are projected to continue in a warming climate (Chang et al., 2012; Kidston & Gerber, 2010; Tamarin-Brodsky & Kaspi, 2017; Chang, 2017; O'Gorman, 2010).

The SH storm track is closely connected with the Southern Annular Mode (SAM) – the SAM is an atmospheric phenomenon, essentially defined as the meridional wandering of the storm track. Campbell and Renwick (2023b) find it organises connections between circulation anomalies and storm activity in the SH, whilst others document feedbacks that, for instance, drive the storm tracks meridionally-defined nature, and persistence in a given SAM mode (Kidston et al., 2010; Lorenz & Hartmann, 2001). The SAM has exhibited a positive trend over the past several decades, driven by increased atmospheric greenhouse gas concentrations (GGCs) and stratospheric ozone depletion. Banerjee et al. (2020) find the trend has ceased since 2000 due to the recovering Antarctic ozone hole; however, continuing greenhouse gas emissions are expected to push the positive trend (Fogt & Marshall, 2020; Arblaster et al., 2011). Knowledge of SAM projections grants insight into the behaviour of the storm track.

Table 1. CMIP6 models with nominal resolution and use of explicit atmospheric chemistry.

Model Name	Resolution (km)	Explicit Ozone
ACCESS-CM2	250	No
ACCESS-ESM1-5	250	No
BCC-CSM2-MR	100	No
CESM2-WACCM	100	Yes
CMCC-CM2-SR5	100	Yes**
CMCC-ESM2	100	Yes**
EC-Earth3	100	No
GFDL-ESM4	100	Yes
NESM3	250	No
NorESM2-MM	100	Yes*

* Prescribed from CESM2-WACCM experiments.
* Fed by high-top simulations with full chemistry.

Projecting a future climatology

Model realisations of scenario experiments evolve according to assumed future climate forcings, natural and anthropogenic. Anthropogenic forcings are uncertain and liable to change alongside societal developments; therefore, plausible scenarios must be assumed. These are captured by combining narratives of societal development – Shared Socioeconomic Pathways (SSPs) (O'Neill et al., 2017) – with a net radiative forcing – Representative Concentration Pathways (RCPs). We investigate two scenarios in this study: SSP1-2.6 (van Vuuren et al., 2017); and SSP5-8.5 (Kriegler et al., 2017). Both scenarios assume similar societal evolution; however, they assume two vastly different CO_2 emissions scenarios, which highlight disparities in the Earth's climate at the end of the 21st century. Although both scenarios are unlikely based on recent societal developments, they provide upper and lower bounds for potential changes. The aim of this study is to qualitatively characterise outcomes at extreme ends of the spectrum.

Study aims

Understanding how SH ST climatology might change is of vital importance for projecting changes to regional climate, and is critical to adopting effective mitigation and adaptation strategies at the local and international level. This study aims to gauge whether general characteristics of the storm track observably change under best- and worst-case scenarios. We build on the work of previous studies to determine whether documented projections persist in the CMIP6 generation of models. We use data from an ensemble of ScenarioMIP models (Table 1). We consider whether robust changes occur in the basic state of the 500hPa geopotential height field (Z500), or its associated high-frequency (HF) variance by the end of the 21st century, and investigate projections of storm track migration. The SAM has been shown to be the organising principle of storm track variability (Campbell & Renwick, 2023b), and CMIP6 models capture this relationship well (Campbell & Renwick, 2023a); therefore, we investigate spatio-temporal changes in the SAM. Our methodology is detailed in section 2. Section 3 presents projections with a focus on the ensemble means, followed by a discussion and conclusion in section 4.

2 Methodology and Data

We use data from the SSP1-2.6 and SSP5-8.5 experiments (2070-2099), and corresponding historical experiment (1972-2014), from 10 CMIP6 models, gathered from

the ESGF Node (`https://esgf-node.llnl.gov/search/cmip6/`). We use the Z500 field, and its associated HF variance, isolated using a 2–8-day bandpass filter (Campbell & Renwick, 2023b), as a proxy for storm activity. Data is gridded at 1° latitude-longitude resolution.

Although model democracy has been called into question (Sanderson et al., 2017; Knutti, 2010), there remains no universal technique for weighting models; therefore, model democracy has been adopted. This study is a continuation of Campbell and Renwick (2023a), which investigated the fidelity of CMIP6 models in representing the SH storm track – models considered here are a subset of the models they used. They found models generally perform well, with no clearly superior models. Model selection is here based on several considerations, notably: bias in the storm track strength (Campbell & Renwick, 2023a); and maximising the parameter space by granting precedence to models from differing modelling groups.

Projections of the climatological mean fields for the Z500 field and its associated HF variance are investigated, given the close relationship between the two (Campbell & Renwick, 2023b). To characterise robust projections, we follow the method outlined in Tebaldi et al. (2011), whereby the projected multi-model ensemble (MME) mean field is displayed if some pre-determined number of models agree on sign and statistical significance of change. We calculate significance at the grid cell level using Welch's t-test, combined with the false discovery rate (FDR) method (Wilks, 2016).

Meridional position of the maximum Z500 gradient and maximum HF variance using temporally and zonally averaged fields are used as proxies for storm track position (Campbell & Renwick, 2023a). We use a Common Basis Function (CBF) analysis (Lee et al., 2019) to reconstruct projected SAM spatio-temporal variability. Spatial patterns are constructed by mapping model anomalies onto the leading EOF retrieved from ERA-5 Z500 anomalies south of 20°S (1979-2021), and regressing the subsequent CBF-PC onto anomalies at the grid cell level. Temporal variability is captured by the standard deviation of the CBF-PC, which we use as a proxy for the magnitude of SAM events. Explained variance (EV) provides a metric for the importance of a given mode; this is defined as the ratio between the area-weighted temporal variance of a reconstructed spatio-temporal field and that of the full field, as per Lee et al. (2019).

3 Results

3.1 Climatological Fields Projections

Figure 1a shows changes from the historical period in the Z500 field are significant and robust at all grid cells south of 20°S in both scenarios. These changes are much exaggerated in SSP5-8.5, reaching a maximum change of around $120m$, whereas a maximum change of $45m$ is recorded for SSP1-2.6. Z500 mean height increases across the hemisphere, with greater changes over the tropics and lesser changes over higher latitudes (particularly clear in SSP5-8.5, Figure 1a). This is likely a signal of warming temperatures and associated expansion of air columns – exaggerated at lower latitudes – increasing the depth of the troposphere. The differential change between the mid-latitudes and adjacent higher latitudes would suggest steeper meridional gradients are to be expected, hence increased mean available potential energy (MAPE) (O'Gorman, 2010). Maximum Z500 changes occur in a broken ring around the mid-latitudes, equatorward of the storm track meridional location, strongest in a band stretching from the Indian Ocean, across Australia to the central Pacific (Figure 1a, SSP5-8.5).

Similarly, both scenarios have similar spatial patterns of change in the HF variance field, with SSP5-8.5 exaggerated (Figure 1b). The signal in SSP1-2.6 is less pronounced – less than 50% of models identified significance at any grid cell, whereas SSP5-8.5 has large regions of significance. There is a lack of consensus on the direction of change in
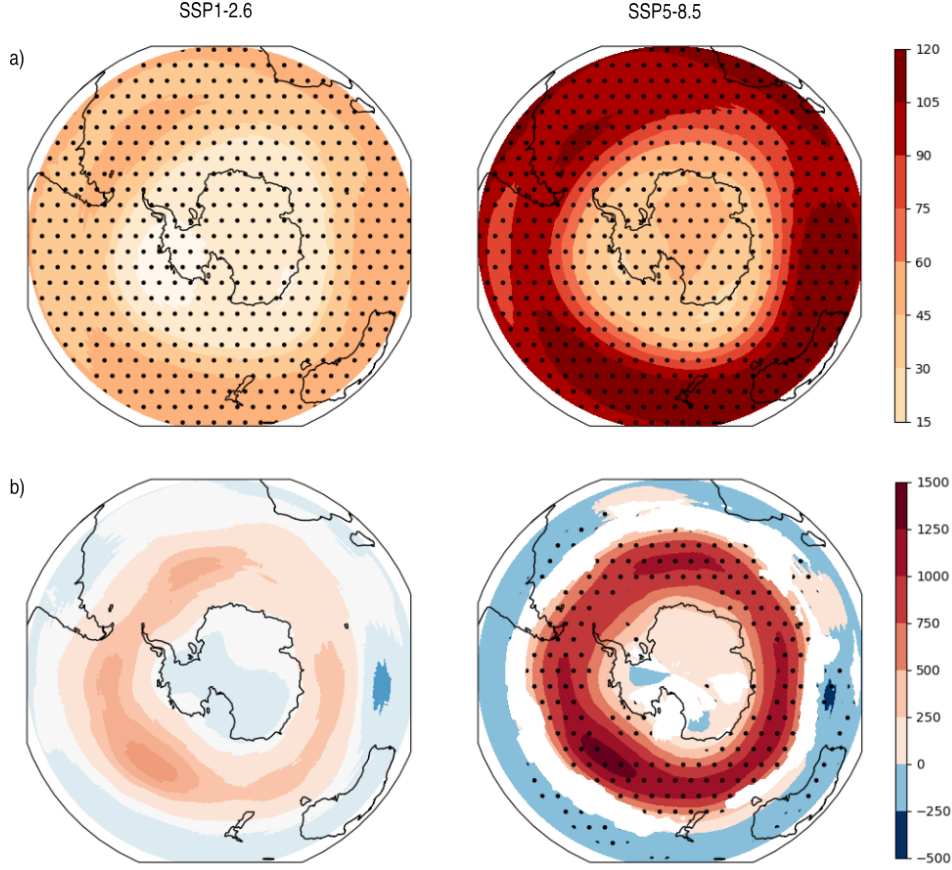
Figure 1. Difference from historical climatological mean state for Z500 and HF variance fields for each scenario ensemble mean at the end of the 21st century. Colour fill designates a change with fewer than 50% of models identifying significance at the grid cell level. Stippling indicates a change with over 50% of models finding significance, and at least 80% of significant models in agreement on the direction of change. Grid cells where there is greater than 50% significance, but less than 80% consensus on the direction of change, are marked in white.

some regions in SSP5-8.5, around the flanks of the storm track (marked as white space in Figure 1b). The strongest changes occur over the storm track, with the greatest increase in storm activity arising over the Pacific – previously noted to be relatively weaker than maxima over the Indian and Atlantic oceans (Campbell & Renwick, 2023b; Hoskins & Hodges, 2005). This might be linked to the higher Z500 field around Australia, as meridional gradients will be sharper in this region with a greater height increase. The consensus between scenarios would suggest a more active storm track is expected in the future, in agreement with previous studies (O'Gorman, 2010; Chang, 2017; Chemke et al., 2022).

3.2 Storm Track Meridional Position

Figure 2 shows the meridional profiles for both scenarios, with peak positions for the historical and scenario ensemble means indicated. The meridional profiles of the historical and SSP1-2.6 ensemble means are almost indistinguishable in both fields (Figure 2), with peak positions within 0.2° in each case, with comparable peak amplitudes, suggesting no clear changes from the historical period arise under a low-emissions scenario.
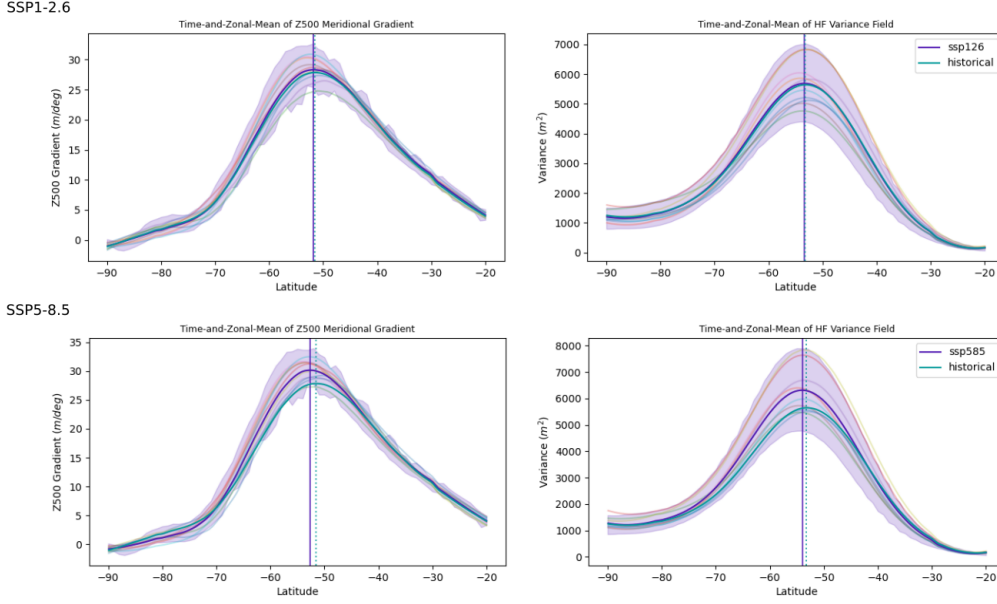
Figure 2. Meridional profiles for mean Z500 gradient and HF variance derived from time- and zonal-mean fields. Vertical lines mark peak positions for scenario and CMIP6 historical ensemble means. Shading indicates two standard errors.

For SSP5-8.5, there is a consistent but small poleward shift – 1.0° for the Z500 gradient peak, 0.8° in the HF variance peak – relative to the historical period (Figure 2). The meridional profiles are highly similar, with peak amplitudes the most significant difference. Amplitude of the HF variance peak increases in accordance with increased storm activity (Figure 1), but fails to reach the peak zonal-mean HF variance of ERA-5, documented by Campbell and Renwick (2023a). Changes in amplitude fall within inter-model uncertainty, but almost all models predict a higher peak than the historical experiment ensemble mean, indicating a degree of robustness.

A poleward shift coincides with increasing peak amplitude in the Z500 meridional gradient (Figure 2). This may be a signal of increased westerlies occurring with greater SAM amplitude, or related to increased momentum convergence with greater storm activity, combined with the poleward propagation bias of storms. Alternatively, as the storm track moves poleward, conservation of angular momentum implies stronger westerlies will result.

The peak shifts are not found to be statistically significant; however, the magnitudes agree with the findings of Kidston and Gerber (2010) for the CMIP3 SRES A2 ex-

Table 2. Peak positions of maximum Z500 meridional gradient and high-frequency variance of CMIP6 historical, SSP1-2.6, and SSP5-8.5 experiment ensemble means, using temporally and zonally averaged fields.

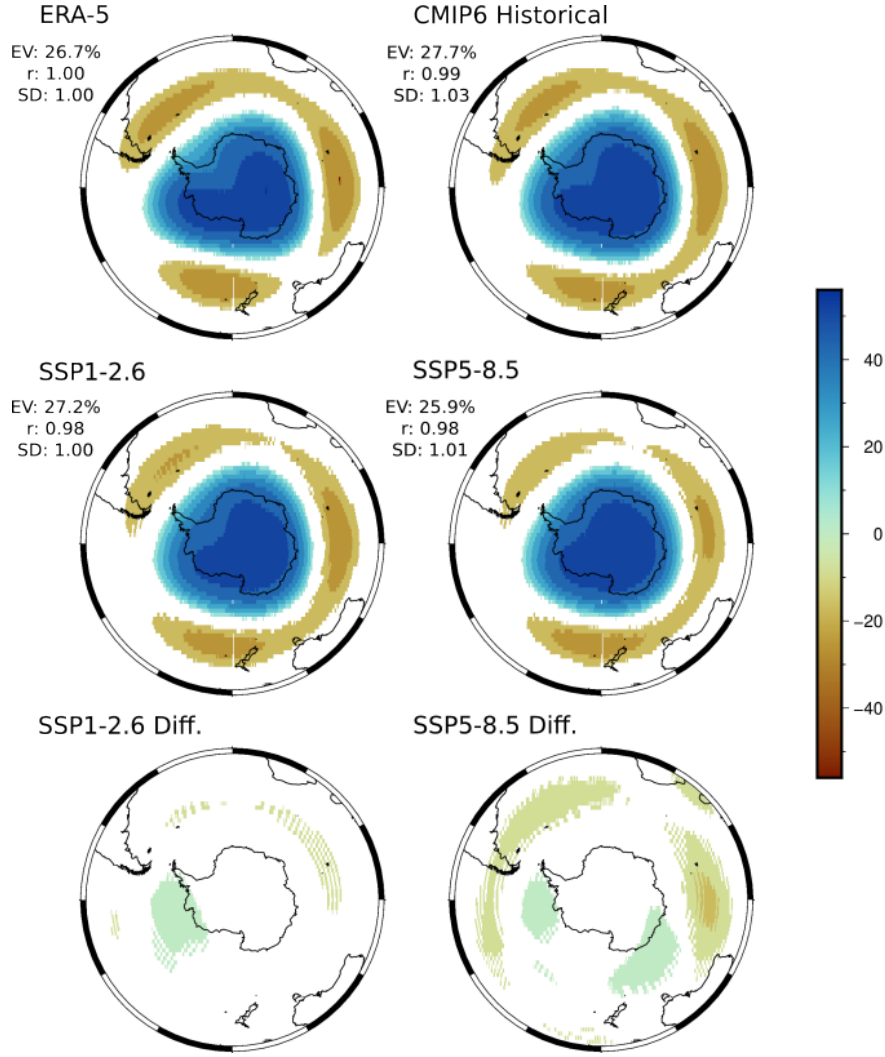| Experiment	Z500 Gradient (°S)	HF Variance (°S)
Historical	51.6	53.2
SSP1-2.6	51.8	53.4
SSP5-8.5	52.6	54.0

Figure 3. Ensemble mean SAM CBFs for CMIP6 historical experiment, SSP1-2.6 and SSP5-8.5 projections, and reference ERA-5 EOF. Explained variance (EV), pattern correlation (r), and normalised CBF-PC temporal SD are provided. The bottom row presents differences from the historical experiment for SSP1-2.6 and SSP5-8.5 projections.

periment (similar to the RCP8.5 and SSP5-8.5 scenarios). The authors find enhanced poleward propagation in some models was due to an equatorward bias in the base state; however, previous studies indicate the equatorward bias is largely neutralised for CMIP6 (Bracegirdle et al., 2020; Priestley et al., 2020; Campbell & Renwick, 2023a). In contrast to Revell et al. (2022), explicit representation of ozone did not seem to have an effect on peak position. The neutralised bias provides confidence that projected changes are likely physical, and is consistent with the documented relationship of greenhouse gas concentrations pushing a poleward storm track (Arblaster et al., 2011). The poleward shift in both fields might indicate the source of the shift is baroclinic in nature.

3.3 Southern Annular Mode Spatio-Temporal Variability

Figure 3 presents the reconstructed SAM spatial patterns for the ensemble mean of both scenarios, the historical experiment, and the ERA-5 EOF. Results suggest pro-

jected SAM spatio-temporal variability remains relatively constant. Consistently high pattern correlations and explained variances indicate the SAM remains a dominant mode of variability, with a largely similar spatial structure. The amplitudes of the spatial patterns are consistent with the ERA-5 reference EOF, and the temporal variability (quantified as CBF-PC temporal standard deviation (SD)) is similarly comparable. The more symmetrical picture provided by the experiment ensembles – note the more prominent asymmetrical protrusion over the Pacific mid-latitudes in ERA-5 (Figure 3) – appears to be a systematic model bias. Consistent temporal SD across experiments (Figure 3) indicates SAM amplitudes remain similar. CBF-PC distributions (not shown) were investigated but suggest no clear changes to SAM behaviour. Although significance may be established with a larger ensemble, these results suggest that despite the poleward migration of the storm track, the wandering behaviour remains similar to the historical period.

The EV of the historical experiment appears to overestimate the importance of the SAM, with 27.7%, as opposed to the 26.7% of ERA-5. This decreases to a value of 25.9% for the SSP5-8.5 ensemble mean, possibly indicating the SAM becomes less of a controlling influence under a high-emissions scenario, perhaps due to increased influence of other sources of variability; however, significance was not established. Differences from the historical experiment are presented in Figure 3. There appears to be a consistent change over the mid-latitude Indian Ocean. The difference grows considerably between scenario projections, $-4.3m$ (7.6% of historical ensemble mean amplitude) in SSP1-2.6, and $-8.7m$ (15%) in SSP5-8.5. This suggests variance over the Indian Ocean related to the SAM decreases with increased emissions, which may contribute to the corresponding diminished EV.

The ensemble spread of EV and SD is greater in the high-emissions scenario, 53% and 49% more than the historical experiment. SSP1-2.6 has lower spread, at 9% and 5% for EV and SD, suggesting model projections diverge as the Earth's basic state is forced further from the familiar conditions under which empirical relationships were derived. Removing the constraining influence of observations and tuning targets inherent in the historical experiment makes disparate projections more likely.

4 Discussion & Conclusion

Changes to the climatological mean fields under high- and low-emissions scenarios strongly suggest the storm track will intensify with continued anthropogenic forcing – the same pattern of changes are identified in both scenarios, though these are stronger under the high-emissions scenario – reinforcing previously documented projections (O'Gorman, 2010; Chang, 2017). The largest increase in storm activity occurs in the central mid-latitude Pacific, downstream of the greatest increase in Z500 mean height. The baroclinic relationship highlighted in Campbell and Renwick (2023a, 2023b), would suggest the two are linked by the downstream development process. Differential changes in Z500 height between low and high latitudes indicates meridional Z500 gradients will strengthen, increasing baroclinicity, hence drive increased storm track activity.

Our results reaffirm the poleward shift in the SH storm track climatological position under a high-emissions scenario, in agreement with studies on previous CMIP generations (Kidston & Gerber, 2010; Tamarin-Brodsky & Kaspi, 2017; Chang, 2017). The neutralised bias in the CMIP6 generation (Bracegirdle et al., 2020; Priestley et al., 2020; Campbell & Renwick, 2023a) allows a degree of confidence in the robustness of this result. The amplitude of the Z500 meridional gradient and HF variance peaks similarly increase, in line with projected increased climatological Z500 height and storm activity. Minimal changes to peak positions and amplitudes were found for the low-emissions scenario.

Revell et al. (2022) find models with no explicit stratospheric ozone chemistry project a much stronger westerly jet, due to their use of outdated forcing datasets from CMIP5 RCPs. No clear distinction between models with and without explicit chemistry could be made here in projected magnitude of maximum zonal-mean Z500 meridional gradients and HF variance, nor peak positions.

Few changes from the historical SAM behaviour could be identified, with pattern correlation and temporal variability remaining largely the same. This suggests models predict the structure and scale of SAM events remain relatively constant, thus little change to the meridional wandering of the storm track. A region of consistent change occurs over the Indian Ocean, with a decrease of $8.7m$ in the high-emissions scenario CBF from the historical, 15% of the historical experiment ensemble mean amplitude. Drivers of this result is left to a future study.

Despite robust results, projections of storm track amplitude remain uncertain due to the presence of considerable systematic biases. The maximum magnitude of the spatial bias noted in Campbell and Renwick (2023a) is twice the greatest change under SSP5-8.5, at $2000m^2$ and $1000m^2$ respectively, and the bias over the Pacific Ocean is roughly equal to the projected change in this sector. These biases may be linked to those identified by (Chemke et al., 2022), who find models do not accurately capture the positive barotropic growth rate trend, nor the momentum convergence around the flanks of the storm track (Kidston et al., 2010). An effort to improve this bias should be made in order to have confidence in projections of storm activity.

Open Research Section

ERA-5 data is freely available from the ECMWF Copernicus Online Data Store at `https://cds.climate.copernicus.eu/cdsapp#!/dataset/reanalysis-era5-pressure-levels?tab=form`. Model output is available at the ESGF Node (`https://esgf-node.llnl.gov/search/cmip6/`), all models used in this study are listed in Table 1.

References

Arblaster, J. M., Meehl, G. A., & Karoly, D. J. (2011). Future climate change in the Southern Hemisphere: Competing effects of ozone and greenhouse gases. *Geophysical Research Letters*, *38*(2), L02701. doi: 10.1029/2010GL045384

Banerjee, A., Fyfe, J. C., Polvani, L. M., Waugh, D., & Chang, K.-L. (2020, March). A pause in Southern Hemisphere circulation trends due to the Montreal Protocol. *Nature*, *579*(7800), 544–548. doi: 10.1038/s41586-020-2120-4

Bracegirdle, T. J., Holmes, C. R., Hosking, J. S., Marshall, G. J., Osman, M., Patterson, M., & Rackow, T. (2020). Improvements in Circumpolar Southern Hemisphere Extratropical Atmospheric Circulation in CMIP6 Compared to CMIP5. *Earth and Space Science*, *7*(6), e2019EA001065. doi: 10.1029/2019EA001065

Campbell, I., & Renwick, J. (2023a). CMIP6 model fidelity in capturing the Southern Hemisphere storm track and its connections with low-frequency variability. *Journal of Geophysical Research: Atmospheres (under review)*.

Campbell, I., & Renwick, J. (2023b). Southern Hemisphere storm tracks and large-scale variability: what do the latest reanalyses say? *Journal of Climate (under review)*.

Chang, E. K. M. (2017, July). Projected Significant Increase in the Number of Extreme Extratropical Cyclones in the Southern Hemisphere. *Journal of Climate*, *30*(13), 4915–4935. doi: 10.1175/JCLI-D-16-0553.1

Chang, E. K. M., Guo, Y., & Xia, X. (2012). CMIP5 multimodel ensemble projection of storm track change under global warming. *Journal of Geophysical Research: Atmospheres*, *117*(D23), D23118. doi: 10.1029/2012JD018578

Chemke, R., Ming, Y., & Yuval, J. (2022, May). The intensification of winter midlatitude storm tracks in the Southern Hemisphere. *Nature Climate Change*, 1–5. doi: 10.1038/s41558-022-01368-8

Eyring, V., Gillett, N., Achuta Rao, K., Barimalala, R., Barreiro Parrillo, M., Bellouin, N., . . . Sun, Y. (2021). Human Influence on the Climate System. In V. Masson-Delmotte et al. (Eds.), *Climate Change 2021: The Physical Science Basis. Contribution of Working Group I to the Sixth Assessment Report of the Intergovernmental Panel on Climate Change* (pp. 423–552). Cambridge, United Kingdom and New York, NY, USA: Cambridge University Press.

Fogt, R. L., & Marshall, G. J. (2020). The Southern Annular Mode: Variability, trends, and climate impacts across the Southern Hemisphere. *WIREs Climate Change*, *11*(4), e652. doi: 10.1002/wcc.652

Hoskins, B. J., & Hodges, K. I. (2005, October). A New Perspective on Southern Hemisphere Storm Tracks. *Journal of Climate*, *18*(20), 4108–4129. doi: 10.1175/JCLI3570.1

Kidston, J., Frierson, D. M. W., Renwick, J. A., & Vallis, G. K. (2010, December). Observations, Simulations, and Dynamics of Jet Stream Variability and Annular Modes. *Journal of Climate*, *23*(23), 6186–6199. doi: 10.1175/2010JCLI3235.1

Kidston, J., & Gerber, E. P. (2010). Intermodel variability of the poleward shift of the austral jet stream in the CMIP3 integrations linked to biases in 20th century climatology. *Geophysical Research Letters*, *37*(9), L09708. doi: 10.1029/2010GL042873

Knutti, R. (2010, October). The end of model democracy? *Climatic Change*, *102*(3), 395–404. doi: 10.1007/s10584-010-9800-2

Kriegler, E., Bauer, N., Popp, A., Humpenöder, F., Leimbach, M., Strefler, J., . . . Edenhofer, O. (2017, January). Fossil-fueled development (SSP5): An energy and resource intensive scenario for the 21st century. *Global Environmental Change*, *42*, 297–315. doi: 10.1016/j.gloenvcha.2016.05.015

Lee, J., Sperber, K. R., Gleckler, P. J., Bonfils, C. J. W., & Taylor, K. E. (2019, April). Quantifying the agreement between observed and simulated extratropical modes of interannual variability. *Climate Dynamics*, *52*(7), 4057–4089. doi: 10.1007/s00382-018-4355-4

Lorenz, D. J., & Hartmann, D. L. (2001, November). Eddy–Zonal Flow Feedback in the Southern Hemisphere. *Journal of the Atmospheric Sciences*, *58*(21), 3312–3327. doi: 10.1175/1520-0469(2001)058⟨3312:EZFFIT⟩2.0.CO;2

O'Gorman, P. A. (2010, November). Understanding the varied response of the extratropical storm tracks to climate change. *Proceedings of the National Academy of Sciences*, *107*(45), 19176–19180. doi: 10.1073/pnas.1011547107

O'Neill, B. C., Kriegler, E., Ebi, K. L., Kemp-Benedict, E., Riahi, K., Rothman, D. S., . . . Solecki, W. (2017, January). The roads ahead: Narratives for shared socioeconomic pathways describing world futures in the 21st century. *Global Environmental Change*, *42*, 169–180. doi: 10.1016/j.gloenvcha.2015.01.004

Pena-Ortiz, C., Gallego, D., Ribera, P., Ordonez, P., & Alvarez-Castro, M. D. C. (2013). Observed trends in the global jet stream characteristics during the second half of the 20th century. *Journal of Geophysical Research: Atmospheres*, *118*(7), 2702–2713. doi: 10.1002/jgrd.50305

Pfahl, S., & Wernli, H. (2012, October). Quantifying the Relevance of Cyclones for Precipitation Extremes. *Journal of Climate*, *25*(19), 6770–6780. doi: 10.1175/

JCLI-D-11-00705.1

Priestley, M. D. K., Ackerley, D., Catto, J. L., Hodges, K. I., McDonald, R. E., & Lee, R. W.   (2020, August).   An Overview of the Extratropical Storm Tracks in CMIP6 Historical Simulations. *Journal of Climate*, *33*(15), 6315–6343. doi: 10.1175/JCLI-D-19-0928.1

Reboita, M. S., da Rocha, R. P., Ambrizzi, T., & Gouveia, C. D.   (2015, October). Trend and teleconnection patterns in the climatology of extratropical cyclones over the Southern Hemisphere.   *Climate Dynamics*, *45*(7), 1929–1944.   doi: 10.1007/s00382-014-2447-3

Revell, L. E., Robertson, F., Douglas, H., Morgenstern, O., & Frame, D. (2022). Influence of Ozone Forcing on 21st Century Southern Hemisphere Surface Westerlies in CMIP6 Models. *Geophysical Research Letters*, *49*(6), e2022GL098252. doi: 10.1029/2022GL098252

Sanderson, B. M., Wehner, M., & Knutti, R.   (2017, June).   Skill and independence weighting for multi-model assessments.   *Geoscientific Model Development*, *10*(6), 2379–2395. doi: 10.5194/gmd-10-2379-2017

Tamarin-Brodsky, T., & Kaspi, Y. (2017, December).   Enhanced poleward propagation of storms under climate change. *Nature Geoscience*, *10*(12), 908–913. doi: 10.1038/s41561-017-0001-8

Tebaldi, C., Arblaster, J. M., & Knutti, R. (2011). Mapping model agreement on future climate projections. *Geophysical Research Letters*, *38*(23), L23701. doi: 10.1029/2011GL049863

van Vuuren, D. P., Stehfest, E., Gernaat, D. E. H. J., Doelman, J. C., van den Berg, M., Harmsen, M., . . . Tabeau, A.   (2017, January).   Energy, land-use and greenhouse gas emissions trajectories under a green growth paradigm.   *Global Environmental Change*, *42*, 237–250. doi: 10.1016/j.gloenvcha.2016.05.008

Wang, X. L., Feng, Y., Chan, R., & Isaac, V.   (2016, November).   Inter-comparison of extra-tropical cyclone activity in nine reanalysis datasets.   *Atmospheric Research*, *181*, 133–153. doi: 10.1016/j.atmosres.2016.06.010

Wilks, D. S.   (2016, December).   "The Stippling Shows Statistically Significant Grid Points": How Research Results are Routinely Overstated and Overinterpreted, and What to Do about It.   *Bulletin of the American Meteorological Society*, *97*(12), 2263–2273. doi: 10.1175/BAMS-D-15-00267.1

High- and low-emissions scenario projections of the Southern Hemisphere storm track

I. Campbell[1], J. Renwick[1]

[1]Te Herenga Waka - Victoria, University of Wellington

Key Points:

- We find increased storm track activity across the Southern Hemisphere is projected to scale with emissions.
- Similar to previous generations, CMIP6 models predict a poleward migration of the Southern Hemisphere storm track.
- The role of the Southern Annular Mode doesn't change significantly with continued anthropogenic forcing.

Corresponding author: Isaac Campbell, `isaac.campbell6@googlemail.com`

Abstract

The Southern Hemisphere storm track is a key component of the Earth's global circulation patterns, with a prominent role in the movement of heat and momentum across the mid-latitudes, and a controlling influence over the behaviour of synoptic eddies. Storm track characteristics are expected to change with anthropogenic forcings, leading to changes in regional weather patterns, and impacting communities through its influence on extreme events. We document projected storm track climatologies at the end of the 21st century under high- and low-emissions scenarios using the CMIP6 generation of models. We find previously described projections – the poleward migration of the storm track, and intensification of storm activity – persist in CMIP6. We explore projections of spatio-temporal variability of the Southern Annular Mode, and consequences for the storm track.

Plain Language Summary

Weather in the Southern Hemisphere is heavily influenced by the storm track, with extreme events in the mid-latitudes closely linked to passing storms. As the Earth's climate changes with continued greenhouse gas emissions, understanding how the storm track will change is vital to make effective efforts to adapt. We show that state-of-the-art models indicate storm activity is set to increase, likely leading to more frequent extreme weather where storms occur.

1 Introduction

The storm track: past, present, and future

The global climate is a complex system; a web of tensions and feedbacks that make its evolution difficult to predict in detail. The Earth's climate tends toward a state of equilibrium; however, human-induced changes have caused a shift in the basic state (Eyring et al., 2021). Primarily, CO_2 emissions alter atmospheric chemistry, leading to an altered radiative budget. As the climate tends toward a new equilibrium, forced changes will impact components of the Earth system, such as the storm tracks.

The Southern Hemisphere (SH) storm track influences hemispheric circulation patterns, and properties of synoptic eddies, which directly impact human lives and livelihoods (Pfahl & Wernli, 2012). Storm track characteristics exhibit trends over the historical record. Several studies suggest there has been a poleward migration of the mean storm track position (Pena-Ortiz et al., 2013), an increase in the extreme storm frequency (Reboita et al., 2015; Wang et al., 2016), and in eddy kinetic energy (EKE) (Chemke et al., 2022). Studies find these trends are projected to continue in a warming climate (Chang et al., 2012; Kidston & Gerber, 2010; Tamarin-Brodsky & Kaspi, 2017; Chang, 2017; O'Gorman, 2010).

The SH storm track is closely connected with the Southern Annular Mode (SAM) – the SAM is an atmospheric phenomenon, essentially defined as the meridional wandering of the storm track. Campbell and Renwick (2023b) find it organises connections between circulation anomalies and storm activity in the SH, whilst others document feedbacks that, for instance, drive the storm tracks meridionally-defined nature, and persistence in a given SAM mode (Kidston et al., 2010; Lorenz & Hartmann, 2001). The SAM has exhibited a positive trend over the past several decades, driven by increased atmospheric greenhouse gas concentrations (GGCs) and stratospheric ozone depletion. Banerjee et al. (2020) find the trend has ceased since 2000 due to the recovering Antarctic ozone hole; however, continuing greenhouse gas emissions are expected to push the positive trend (Fogt & Marshall, 2020; Arblaster et al., 2011). Knowledge of SAM projections grants insight into the behaviour of the storm track.

Table 1. CMIP6 models with nominal resolution and use of explicit atmospheric chemistry.

Model Name	Resolution (km)	Explicit Ozone
ACCESS-CM2	250	No
ACCESS-ESM1-5	250	No
BCC-CSM2-MR	100	No
CESM2-WACCM	100	Yes
CMCC-CM2-SR5	100	Yes**
CMCC-ESM2	100	Yes**
EC-Earth3	100	No
GFDL-ESM4	100	Yes
NESM3	250	No
NorESM2-MM	100	Yes*

* Prescribed from CESM2-WACCM experiments.
* Fed by high-top simulations with full chemistry.

Projecting a future climatology

Model realisations of scenario experiments evolve according to assumed future climate forcings, natural and anthropogenic. Anthropogenic forcings are uncertain and liable to change alongside societal developments; therefore, plausible scenarios must be assumed. These are captured by combining narratives of societal development – Shared Socioeconomic Pathways (SSPs) (O'Neill et al., 2017) – with a net radiative forcing – Representative Concentration Pathways (RCPs). We investigate two scenarios in this study: SSP1-2.6 (van Vuuren et al., 2017); and SSP5-8.5 (Kriegler et al., 2017). Both scenarios assume similar societal evolution; however, they assume two vastly different CO_2 emissions scenarios, which highlight disparities in the Earth's climate at the end of the 21st century. Although both scenarios are unlikely based on recent societal developments, they provide upper and lower bounds for potential changes. The aim of this study is to qualitatively characterise outcomes at extreme ends of the spectrum.

Study aims

Understanding how SH ST climatology might change is of vital importance for projecting changes to regional climate, and is critical to adopting effective mitigation and adaptation strategies at the local and international level. This study aims to gauge whether general characteristics of the storm track observably change under best- and worst-case scenarios. We build on the work of previous studies to determine whether documented projections persist in the CMIP6 generation of models. We use data from an ensemble of ScenarioMIP models (Table 1). We consider whether robust changes occur in the basic state of the 500hPa geopotential height field (Z500), or its associated high-frequency (HF) variance by the end of the 21st century, and investigate projections of storm track migration. The SAM has been shown to be the organising principle of storm track variability (Campbell & Renwick, 2023b), and CMIP6 models capture this relationship well (Campbell & Renwick, 2023a); therefore, we investigate spatio-temporal changes in the SAM. Our methodology is detailed in section 2. Section 3 presents projections with a focus on the ensemble means, followed by a discussion and conclusion in section 4.

2 Methodology and Data

We use data from the SSP1-2.6 and SSP5-8.5 experiments (2070-2099), and corresponding historical experiment (1972-2014), from 10 CMIP6 models, gathered from

the ESGF Node (`https://esgf-node.llnl.gov/search/cmip6/`). We use the Z500 field, and its associated HF variance, isolated using a 2–8-day bandpass filter (Campbell & Renwick, 2023b), as a proxy for storm activity. Data is gridded at 1° latitude-longitude resolution.

Although model democracy has been called into question (Sanderson et al., 2017; Knutti, 2010), there remains no universal technique for weighting models; therefore, model democracy has been adopted. This study is a continuation of Campbell and Renwick (2023a), which investigated the fidelity of CMIP6 models in representing the SH storm track – models considered here are a subset of the models they used. They found models generally perform well, with no clearly superior models. Model selection is here based on several considerations, notably: bias in the storm track strength (Campbell & Renwick, 2023a); and maximising the parameter space by granting precedence to models from differing modelling groups.

Projections of the climatological mean fields for the Z500 field and its associated HF variance are investigated, given the close relationship between the two (Campbell & Renwick, 2023b). To characterise robust projections, we follow the method outlined in Tebaldi et al. (2011), whereby the projected multi-model ensemble (MME) mean field is displayed if some pre-determined number of models agree on sign and statistical significance of change. We calculate significance at the grid cell level using Welch's t-test, combined with the false discovery rate (FDR) method (Wilks, 2016).

Meridional position of the maximum Z500 gradient and maximum HF variance using temporally and zonally averaged fields are used as proxies for storm track position (Campbell & Renwick, 2023a). We use a Common Basis Function (CBF) analysis (Lee et al., 2019) to reconstruct projected SAM spatio-temporal variability. Spatial patterns are constructed by mapping model anomalies onto the leading EOF retrieved from ERA-5 Z500 anomalies south of 20°S (1979-2021), and regressing the subsequent CBF-PC onto anomalies at the grid cell level. Temporal variability is captured by the standard deviation of the CBF-PC, which we use as a proxy for the magnitude of SAM events. Explained variance (EV) provides a metric for the importance of a given mode; this is defined as the ratio between the area-weighted temporal variance of a reconstructed spatio-temporal field and that of the full field, as per Lee et al. (2019).

3 Results

3.1 Climatological Fields Projections

Figure 1a shows changes from the historical period in the Z500 field are significant and robust at all grid cells south of 20°S in both scenarios. These changes are much exaggerated in SSP5-8.5, reaching a maximum change of around $120m$, whereas a maximum change of $45m$ is recorded for SSP1-2.6. Z500 mean height increases across the hemisphere, with greater changes over the tropics and lesser changes over higher latitudes (particularly clear in SSP5-8.5, Figure 1a). This is likely a signal of warming temperatures and associated expansion of air columns – exaggerated at lower latitudes – increasing the depth of the troposphere. The differential change between the mid-latitudes and adjacent higher latitudes would suggest steeper meridional gradients are to be expected, hence increased mean available potential energy (MAPE) (O'Gorman, 2010). Maximum Z500 changes occur in a broken ring around the mid-latitudes, equatorward of the storm track meridional location, strongest in a band stretching from the Indian Ocean, across Australia to the central Pacific (Figure 1a, SSP5-8.5).

Similarly, both scenarios have similar spatial patterns of change in the HF variance field, with SSP5-8.5 exaggerated (Figure 1b). The signal in SSP1-2.6 is less pronounced – less than 50% of models identified significance at any grid cell, whereas SSP5-8.5 has large regions of significance. There is a lack of consensus on the direction of change in
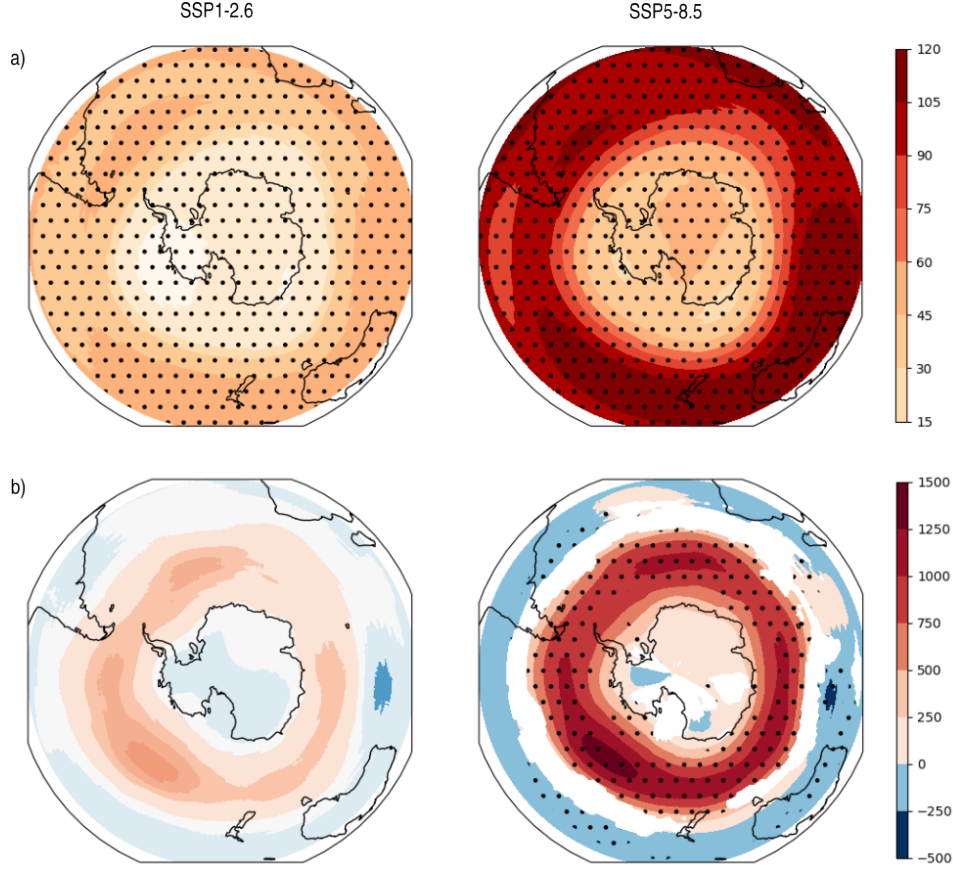
Figure 1. Difference from historical climatological mean state for Z500 and HF variance fields for each scenario ensemble mean at the end of the 21st century. Colour fill designates a change with fewer than 50% of models identifying significance at the grid cell level. Stippling indicates a change with over 50% of models finding significance, and at least 80% of significant models in agreement on the direction of change. Grid cells where there is greater than 50% significance, but less than 80% consensus on the direction of change, are marked in white.

some regions in SSP5-8.5, around the flanks of the storm track (marked as white space in Figure 1b). The strongest changes occur over the storm track, with the greatest increase in storm activity arising over the Pacific – previously noted to be relatively weaker than maxima over the Indian and Atlantic oceans (Campbell & Renwick, 2023b; Hoskins & Hodges, 2005). This might be linked to the higher Z500 field around Australia, as meridional gradients will be sharper in this region with a greater height increase. The consensus between scenarios would suggest a more active storm track is expected in the future, in agreement with previous studies (O'Gorman, 2010; Chang, 2017; Chemke et al., 2022).

3.2 Storm Track Meridional Position

Figure 2 shows the meridional profiles for both scenarios, with peak positions for the historical and scenario ensemble means indicated. The meridional profiles of the historical and SSP1-2.6 ensemble means are almost indistinguishable in both fields (Figure 2), with peak positions within 0.2° in each case, with comparable peak amplitudes, suggesting no clear changes from the historical period arise under a low-emissions scenario.
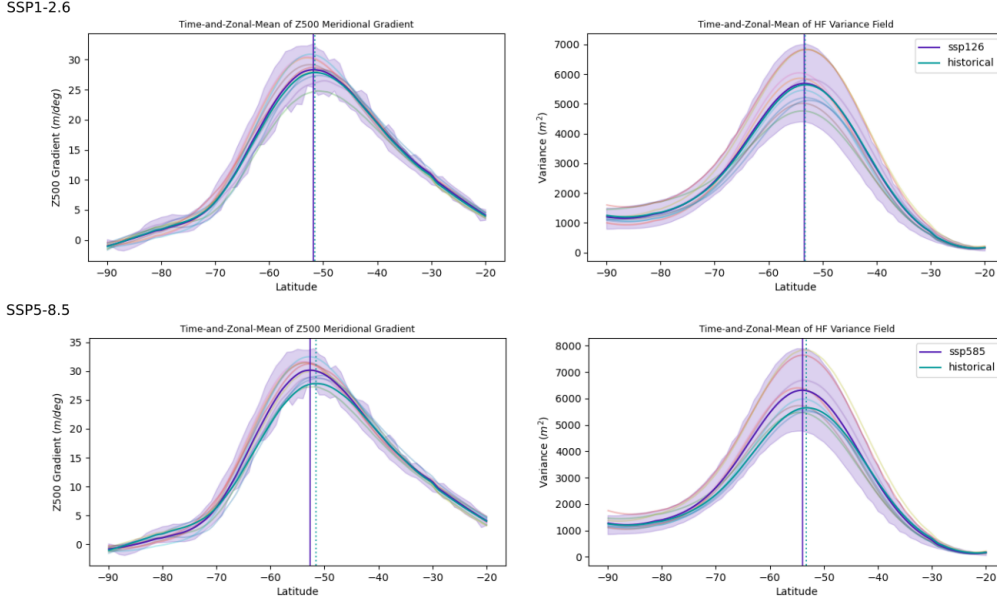
SSP1-2.6

SSP5-8.5

Figure 2. Meridional profiles for mean Z500 gradient and HF variance derived from time- and zonal-mean fields. Vertical lines mark peak positions for scenario and CMIP6 historical ensemble means. Shading indicates two standard errors.

For SSP5-8.5, there is a consistent but small poleward shift – 1.0° for the Z500 gradient peak, 0.8° in the HF variance peak – relative to the historical period (Figure 2). The meridional profiles are highly similar, with peak amplitudes the most significant difference. Amplitude of the HF variance peak increases in accordance with increased storm activity (Figure 1), but fails to reach the peak zonal-mean HF variance of ERA-5, documented by Campbell and Renwick (2023a). Changes in amplitude fall within inter-model uncertainty, but almost all models predict a higher peak than the historical experiment ensemble mean, indicating a degree of robustness.

A poleward shift coincides with increasing peak amplitude in the Z500 meridional gradient (Figure 2). This may be a signal of increased westerlies occurring with greater SAM amplitude, or related to increased momentum convergence with greater storm activity, combined with the poleward propagation bias of storms. Alternatively, as the storm track moves poleward, conservation of angular momentum implies stronger westerlies will result.

The peak shifts are not found to be statistically significant; however, the magnitudes agree with the findings of Kidston and Gerber (2010) for the CMIP3 SRES A2 ex-

Table 2. Peak positions of maximum Z500 meridional gradient and high-frequency variance of CMIP6 historical, SSP1-2.6, and SSP5-8.5 experiment ensemble means, using temporally and zonally averaged fields.

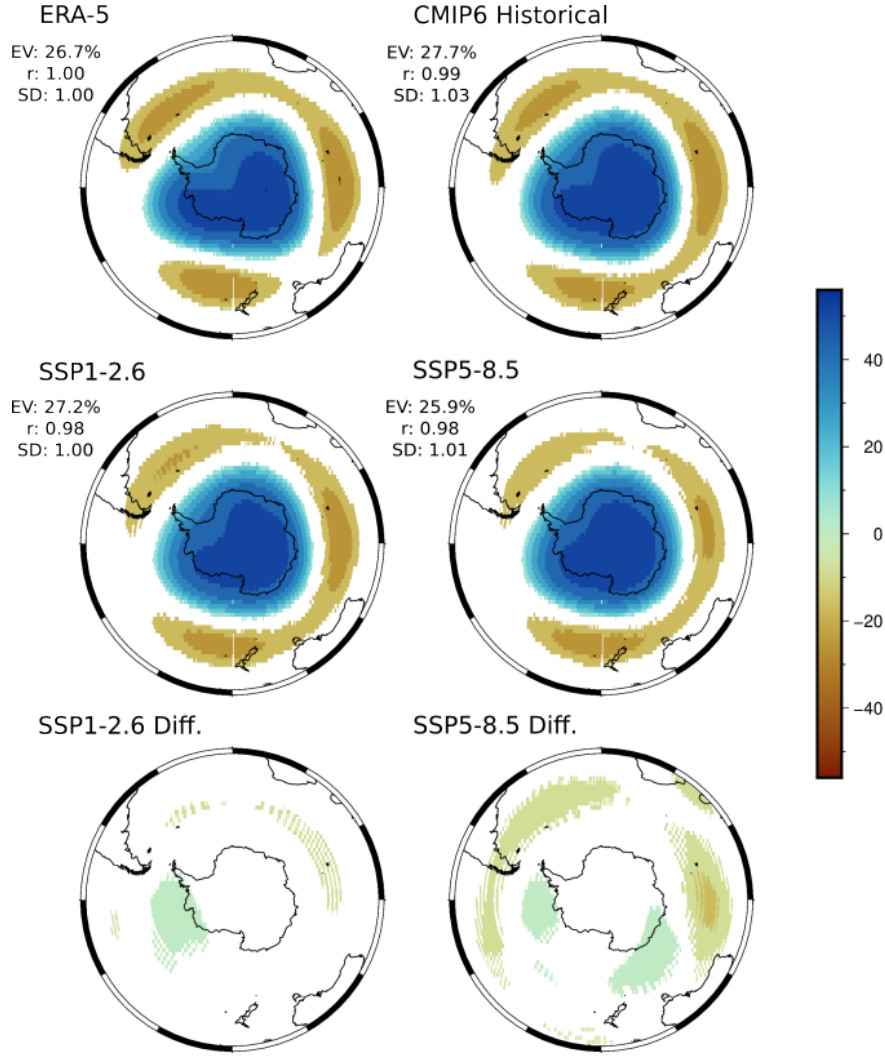| Experiment	Z500 Gradient (°S)	HF Variance (°S)
Historical	51.6	53.2
SSP1-2.6	51.8	53.4
SSP5-8.5	52.6	54.0

Figure 3. Ensemble mean SAM CBFs for CMIP6 historical experiment, SSP1-2.6 and SSP5-8.5 projections, and reference ERA-5 EOF. Explained variance (EV), pattern correlation (r), and normalised CBF-PC temporal SD are provided. The bottom row presents differences from the historical experiment for SSP1-2.6 and SSP5-8.5 projections.

periment (similar to the RCP8.5 and SSP5-8.5 scenarios). The authors find enhanced poleward propagation in some models was due to an equatorward bias in the base state; however, previous studies indicate the equatorward bias is largely neutralised for CMIP6 (Bracegirdle et al., 2020; Priestley et al., 2020; Campbell & Renwick, 2023a). In contrast to Revell et al. (2022), explicit representation of ozone did not seem to have an effect on peak position. The neutralised bias provides confidence that projected changes are likely physical, and is consistent with the documented relationship of greenhouse gas concentrations pushing a poleward storm track (Arblaster et al., 2011). The poleward shift in both fields might indicate the source of the shift is baroclinic in nature.

3.3 Southern Annular Mode Spatio-Temporal Variability

Figure 3 presents the reconstructed SAM spatial patterns for the ensemble mean of both scenarios, the historical experiment, and the ERA-5 EOF. Results suggest pro-

jected SAM spatio-temporal variability remains relatively constant. Consistently high pattern correlations and explained variances indicate the SAM remains a dominant mode of variability, with a largely similar spatial structure. The amplitudes of the spatial patterns are consistent with the ERA-5 reference EOF, and the temporal variability (quantified as CBF-PC temporal standard deviation (SD)) is similarly comparable. The more symmetrical picture provided by the experiment ensembles – note the more prominent asymmetrical protrusion over the Pacific mid-latitudes in ERA-5 (Figure 3) – appears to be a systematic model bias. Consistent temporal SD across experiments (Figure 3) indicates SAM amplitudes remain similar. CBF-PC distributions (not shown) were investigated but suggest no clear changes to SAM behaviour. Although significance may be established with a larger ensemble, these results suggest that despite the poleward migration of the storm track, the wandering behaviour remains similar to the historical period.

The EV of the historical experiment appears to overestimate the importance of the SAM, with 27.7%, as opposed to the 26.7% of ERA-5. This decreases to a value of 25.9% for the SSP5-8.5 ensemble mean, possibly indicating the SAM becomes less of a controlling influence under a high-emissions scenario, perhaps due to increased influence of other sources of variability; however, significance was not established. Differences from the historical experiment are presented in Figure 3. There appears to be a consistent change over the mid-latitude Indian Ocean. The difference grows considerably between scenario projections, $-4.3m$ (7.6% of historical ensemble mean amplitude) in SSP1-2.6, and $-8.7m$ (15%) in SSP5-8.5. This suggests variance over the Indian Ocean related to the SAM decreases with increased emissions, which may contribute to the corresponding diminished EV.

The ensemble spread of EV and SD is greater in the high-emissions scenario, 53% and 49% more than the historical experiment. SSP1-2.6 has lower spread, at 9% and 5% for EV and SD, suggesting model projections diverge as the Earth's basic state is forced further from the familiar conditions under which empirical relationships were derived. Removing the constraining influence of observations and tuning targets inherent in the historical experiment makes disparate projections more likely.

4 Discussion & Conclusion

Changes to the climatological mean fields under high- and low-emissions scenarios strongly suggest the storm track will intensify with continued anthropogenic forcing – the same pattern of changes are identified in both scenarios, though these are stronger under the high-emissions scenario – reinforcing previously documented projections (O'Gorman, 2010; Chang, 2017). The largest increase in storm activity occurs in the central mid-latitude Pacific, downstream of the greatest increase in Z500 mean height. The baroclinic relationship highlighted in Campbell and Renwick (2023a, 2023b), would suggest the two are linked by the downstream development process. Differential changes in Z500 height between low and high latitudes indicates meridional Z500 gradients will strengthen, increasing baroclinicity, hence drive increased storm track activity.

Our results reaffirm the poleward shift in the SH storm track climatological position under a high-emissions scenario, in agreement with studies on previous CMIP generations (Kidston & Gerber, 2010; Tamarin-Brodsky & Kaspi, 2017; Chang, 2017). The neutralised bias in the CMIP6 generation (Bracegirdle et al., 2020; Priestley et al., 2020; Campbell & Renwick, 2023a) allows a degree of confidence in the robustness of this result. The amplitude of the Z500 meridional gradient and HF variance peaks similarly increase, in line with projected increased climatological Z500 height and storm activity. Minimal changes to peak positions and amplitudes were found for the low-emissions scenario.

Revell et al. (2022) find models with no explicit stratospheric ozone chemistry project a much stronger westerly jet, due to their use of outdated forcing datasets from CMIP5 RCPs. No clear distinction between models with and without explicit chemistry could be made here in projected magnitude of maximum zonal-mean Z500 meridional gradients and HF variance, nor peak positions.

Few changes from the historical SAM behaviour could be identified, with pattern correlation and temporal variability remaining largely the same. This suggests models predict the structure and scale of SAM events remain relatively constant, thus little change to the meridional wandering of the storm track. A region of consistent change occurs over the Indian Ocean, with a decrease of $8.7m$ in the high-emissions scenario CBF from the historical, 15% of the historical experiment ensemble mean amplitude. Drivers of this result is left to a future study.

Despite robust results, projections of storm track amplitude remain uncertain due to the presence of considerable systematic biases. The maximum magnitude of the spatial bias noted in Campbell and Renwick (2023a) is twice the greatest change under SSP5-8.5, at $2000m^2$ and $1000m^2$ respectively, and the bias over the Pacific Ocean is roughly equal to the projected change in this sector. These biases may be linked to those identified by (Chemke et al., 2022), who find models do not accurately capture the positive barotropic growth rate trend, nor the momentum convergence around the flanks of the storm track (Kidston et al., 2010). An effort to improve this bias should be made in order to have confidence in projections of storm activity.

Open Research Section

ERA-5 data is freely available from the ECMWF Copernicus Online Data Store at `https://cds.climate.copernicus.eu/cdsapp#!/dataset/reanalysis-era5-pressure-levels?tab=form`. Model output is available at the ESGF Node (`https://esgf-node.llnl.gov/search/cmip6/`), all models used in this study are listed in Table 1.

Acknowledgments

References

Arblaster, J. M., Meehl, G. A., & Karoly, D. J. (2011). Future climate change in the Southern Hemisphere: Competing effects of ozone and greenhouse gases. *Geophysical Research Letters*, *38*(2), L02701. doi: 10.1029/2010GL045384

Banerjee, A., Fyfe, J. C., Polvani, L. M., Waugh, D., & Chang, K.-L. (2020, March). A pause in Southern Hemisphere circulation trends due to the Montreal Protocol. *Nature*, *579*(7800), 544–548. doi: 10.1038/s41586-020-2120-4

Bracegirdle, T. J., Holmes, C. R., Hosking, J. S., Marshall, G. J., Osman, M., Patterson, M., & Rackow, T. (2020). Improvements in Circumpolar Southern Hemisphere Extratropical Atmospheric Circulation in CMIP6 Compared to CMIP5. *Earth and Space Science*, *7*(6), e2019EA001065. doi: 10.1029/2019EA001065

Campbell, I., & Renwick, J. (2023a). CMIP6 model fidelity in capturing the Southern Hemisphere storm track and its connections with low-frequency variability. *Journal of Geophysical Research: Atmospheres (under review)*.

Campbell, I., & Renwick, J. (2023b). Southern Hemisphere storm tracks and large-scale variability: what do the latest reanalyses say? *Journal of Climate (under review)*.

Chang, E. K. M. (2017, July). Projected Significant Increase in the Number of Extreme Extratropical Cyclones in the Southern Hemisphere. *Journal of Climate*, *30*(13), 4915–4935. doi: 10.1175/JCLI-D-16-0553.1

Chang, E. K. M., Guo, Y., & Xia, X. (2012). CMIP5 multimodel ensemble projection of storm track change under global warming. *Journal of Geophysical Research: Atmospheres*, *117*(D23), D23118. doi: 10.1029/2012JD018578

Chemke, R., Ming, Y., & Yuval, J. (2022, May). The intensification of winter midlatitude storm tracks in the Southern Hemisphere. *Nature Climate Change*, 1–5. doi: 10.1038/s41558-022-01368-8

Eyring, V., Gillett, N., Achuta Rao, K., Barimalala, R., Barreiro Parrillo, M., Bellouin, N., . . . Sun, Y. (2021). Human Influence on the Climate System. In V. Masson-Delmotte et al. (Eds.), *Climate Change 2021: The Physical Science Basis. Contribution of Working Group I to the Sixth Assessment Report of the Intergovernmental Panel on Climate Change* (pp. 423–552). Cambridge, United Kingdom and New York, NY, USA: Cambridge University Press.

Fogt, R. L., & Marshall, G. J. (2020). The Southern Annular Mode: Variability, trends, and climate impacts across the Southern Hemisphere. *WIREs Climate Change*, *11*(4), e652. doi: 10.1002/wcc.652

Hoskins, B. J., & Hodges, K. I. (2005, October). A New Perspective on Southern Hemisphere Storm Tracks. *Journal of Climate*, *18*(20), 4108–4129. doi: 10.1175/JCLI3570.1

Kidston, J., Frierson, D. M. W., Renwick, J. A., & Vallis, G. K. (2010, December). Observations, Simulations, and Dynamics of Jet Stream Variability and Annular Modes. *Journal of Climate*, *23*(23), 6186–6199. doi: 10.1175/2010JCLI3235.1

Kidston, J., & Gerber, E. P. (2010). Intermodel variability of the poleward shift of the austral jet stream in the CMIP3 integrations linked to biases in 20th century climatology. *Geophysical Research Letters*, *37*(9), L09708. doi: 10.1029/2010GL042873

Knutti, R. (2010, October). The end of model democracy? *Climatic Change*, *102*(3), 395–404. doi: 10.1007/s10584-010-9800-2

Kriegler, E., Bauer, N., Popp, A., Humpenöder, F., Leimbach, M., Strefler, J., . . . Edenhofer, O. (2017, January). Fossil-fueled development (SSP5): An energy and resource intensive scenario for the 21st century. *Global Environmental Change*, *42*, 297–315. doi: 10.1016/j.gloenvcha.2016.05.015

Lee, J., Sperber, K. R., Gleckler, P. J., Bonfils, C. J. W., & Taylor, K. E. (2019, April). Quantifying the agreement between observed and simulated extratropical modes of interannual variability. *Climate Dynamics*, *52*(7), 4057–4089. doi: 10.1007/s00382-018-4355-4

Lorenz, D. J., & Hartmann, D. L. (2001, November). Eddy–Zonal Flow Feedback in the Southern Hemisphere. *Journal of the Atmospheric Sciences*, *58*(21), 3312–3327. doi: 10.1175/1520-0469(2001)058⟨3312:EZFFIT⟩2.0.CO;2

O'Gorman, P. A. (2010, November). Understanding the varied response of the extratropical storm tracks to climate change. *Proceedings of the National Academy of Sciences*, *107*(45), 19176–19180. doi: 10.1073/pnas.1011547107

O'Neill, B. C., Kriegler, E., Ebi, K. L., Kemp-Benedict, E., Riahi, K., Rothman, D. S., . . . Solecki, W. (2017, January). The roads ahead: Narratives for shared socioeconomic pathways describing world futures in the 21st century. *Global Environmental Change*, *42*, 169–180. doi: 10.1016/j.gloenvcha.2015.01.004

Pena-Ortiz, C., Gallego, D., Ribera, P., Ordonez, P., & Alvarez-Castro, M. D. C. (2013). Observed trends in the global jet stream characteristics during the second half of the 20th century. *Journal of Geophysical Research: Atmospheres*, *118*(7), 2702–2713. doi: 10.1002/jgrd.50305

Pfahl, S., & Wernli, H. (2012, October). Quantifying the Relevance of Cyclones for Precipitation Extremes. *Journal of Climate*, *25*(19), 6770–6780. doi: 10.1175/

JCLI-D-11-00705.1

Priestley, M. D. K., Ackerley, D., Catto, J. L., Hodges, K. I., McDonald, R. E., & Lee, R. W. (2020, August). An Overview of the Extratropical Storm Tracks in CMIP6 Historical Simulations. *Journal of Climate*, *33*(15), 6315–6343. doi: 10.1175/JCLI-D-19-0928.1

Reboita, M. S., da Rocha, R. P., Ambrizzi, T., & Gouveia, C. D. (2015, October). Trend and teleconnection patterns in the climatology of extratropical cyclones over the Southern Hemisphere. *Climate Dynamics*, *45*(7), 1929–1944. doi: 10.1007/s00382-014-2447-3

Revell, L. E., Robertson, F., Douglas, H., Morgenstern, O., & Frame, D. (2022). Influence of Ozone Forcing on 21st Century Southern Hemisphere Surface Westerlies in CMIP6 Models. *Geophysical Research Letters*, *49*(6), e2022GL098252. doi: 10.1029/2022GL098252

Sanderson, B. M., Wehner, M., & Knutti, R. (2017, June). Skill and independence weighting for multi-model assessments. *Geoscientific Model Development*, *10*(6), 2379–2395. doi: 10.5194/gmd-10-2379-2017

Tamarin-Brodsky, T., & Kaspi, Y. (2017, December). Enhanced poleward propagation of storms under climate change. *Nature Geoscience*, *10*(12), 908–913. doi: 10.1038/s41561-017-0001-8

Tebaldi, C., Arblaster, J. M., & Knutti, R. (2011). Mapping model agreement on future climate projections. *Geophysical Research Letters*, *38*(23), L23701. doi: 10.1029/2011GL049863

van Vuuren, D. P., Stehfest, E., Gernaat, D. E. H. J., Doelman, J. C., van den Berg, M., Harmsen, M., . . . Tabeau, A. (2017, January). Energy, land-use and greenhouse gas emissions trajectories under a green growth paradigm. *Global Environmental Change*, *42*, 237–250. doi: 10.1016/j.gloenvcha.2016.05.008

Wang, X. L., Feng, Y., Chan, R., & Isaac, V. (2016, November). Inter-comparison of extra-tropical cyclone activity in nine reanalysis datasets. *Atmospheric Research*, *181*, 133–153. doi: 10.1016/j.atmosres.2016.06.010

Wilks, D. S. (2016, December). "The Stippling Shows Statistically Significant Grid Points": How Research Results are Routinely Overstated and Overinterpreted, and What to Do about It. *Bulletin of the American Meteorological Society*, *97*(12), 2263–2273. doi: 10.1175/BAMS-D-15-00267.1